PROCEEDINGS
OF SCIENCE

ONLINE ICRC 2021
Berlin | Germany
37th International
Cosmic Ray Conference
12–23 July 2021

Reconstruction of Events Recorded with the Water-Cherenkov and Scintillator Surface Detectors of the Pierre Auger Observatory

David Schmidt[a,*] **on behalf of the Pierre Auger**[b] **Collaboration**
(a complete list of authors can be found at the end of the proceedings)

[a]*Institute of Experimental Particle Physics, Karlsruhe Institute of Technology* KIT, *Karlsruhe, Germany*

[b]*Observatorio Pierre Auger, Av. San Martín Norte 304, 5613 Malargüe, Argentina*

E-mail: spokespersons@auger.org

With the knowledge and statistical power of over a decade and a half of measurements, the Auger Collaboration has developed, assessed, and refined robust methods for reconstructing the energies and arrival directions of the highest-energy cosmic rays from the signal and timing measurements of its surface detector array. Concurrently, the unearthing of an increasingly complex astrophysical scenario and tensions with hadronic interaction models have demanded the addition of primary mass as an observable measurable using the surface detector. Access to information on the mass hinges on the disentanglement of the electromagnetic and muonic components of extensive air showers. Consequently, an upgrade to the Observatory, *AugerPrime*, is being carried out by equipping existing water-Cherenkov stations with a $3.8\,\mathrm{m}^2$ Scintillator Surface Detector (SSD). The SSDs, with their high sensitivity to electrons and positrons, will provide samples of the lateral distribution of particles at the ground that complement those of the water-Cherenkov detectors, which are significantly more sensitive to muons. When used together, the two measurements enable extraction of the number of incident muons, which is a quantity that strongly correlates with primary mass. We describe the reconstruction methods being developed for application to measurements of the surface detector of the Observatory with a particular focus on the enhancement of these methods with data of the SSDs of AugerPrime. Results from the reconstruction of thousands of high-energy events already measured with deployed SSDs are also shown.

---

*Presenter

1. Introduction

Prior to the measurements of the Pierre Auger Observatory, the working assumption was that the ultra-high-energy cosmic rays arriving at Earth were purely protons. Precise measurement of the depth of the shower maximum by the fluorescence detectors of the Observatory [1] coupled with better constrained hadronic interaction models at the highest energies have since painted a different picture. To unravel the open questions surrounding the sources of ultra-high-energy cosmic rays and to further study hadronic interactions beyond the reach of man-made colliders, knowledge of the mass composition of the highest energy cosmic rays is required.

Information on the mass composition has thus far been delivered by the measurement of the depth of the shower maximum X_{max} by the fluorescence detector of the Observatory. However, due to its duty cycle of only ~15%, the fluorescence detector provides only limited event statistics in the suppression region of the energy spectrum. Despite a decade and a half of Observatory operation, the number of measurements of X_{max} passing quality cuts for composition analysis amount to fewer than 100 for energies greater than $10^{19.5}$ eV.

The second phase of the Observatory, known as *AugerPrime* [2, 3], consists of equipping the surface detector array, whose duty cycle is nearly 100%, with the hardware necessary to attain sensitivity to primary mass at the highest energies. Scintillator Surface Detectors (SSDs) are being placed on top of the water-Cherenkov detectors (WCDs) in the existing array. The higher sensitivity of the SSD to positrons and electrons complements the more muon-sensitive WCD, and the combined use of the two detectors enables the disentanglement of the contributions of the electromagnetic and muonic shower components in surface detector measurements. As the magnitude of the muonic component of extensive air showers produced by ultra-high-energy cosmic rays scales with mass, sensitivity to primary mass will be achieved in this way.

2. AugerPrime Surface Detector Array

The $3000\,km^2$ surface detector array of the Observatory is located at an elevation of ~1400 m and is comprised of over 1600 surface detector stations arranged on an isometric triangular grid with 1500 m spacing. Once the AugerPrime upgrade is completed, stations in the array will consist of both a WCD and an SSD, with the exception of those on the outer perimeter of the array, where the impact of supplementary scintillator measurements is expected to be smaller.

A schematic of a surface detector station of AugerPrime is depicted in Fig. 1 (*left*). The active volume of a WCD consists of a cylinder of water with a radius of 1.8 m and a depth of 1.2 m. Each SSD has an active area of $3.84\,m^2$ comprised of 48 polystyrene scintillator bars measuring 160 cm by 5 cm with a thickness of 1 cm. A detailed description of the detector materials, geometry, and construction of the WCDs and SSDs may be found in Refs. [4] and [5], respectively. The deployment of production design SSDs began in March of 2019 and is expected to finish by the end of 2021 [6].

Hundreds of thousands of events enhanced with SSD data have already been measured, of which over a thousand have energies greater than $10^{18.5}$ eV and pass quality cuts. A detailed description of the reconstruction algorithms applied to surface detector measurements prior to the addition of the SSD is given in Ref. [7]. In this proceeding, we will detail the methods applied to SSD measurements on the level of individual detectors (Section 3) and the event (Section 4).
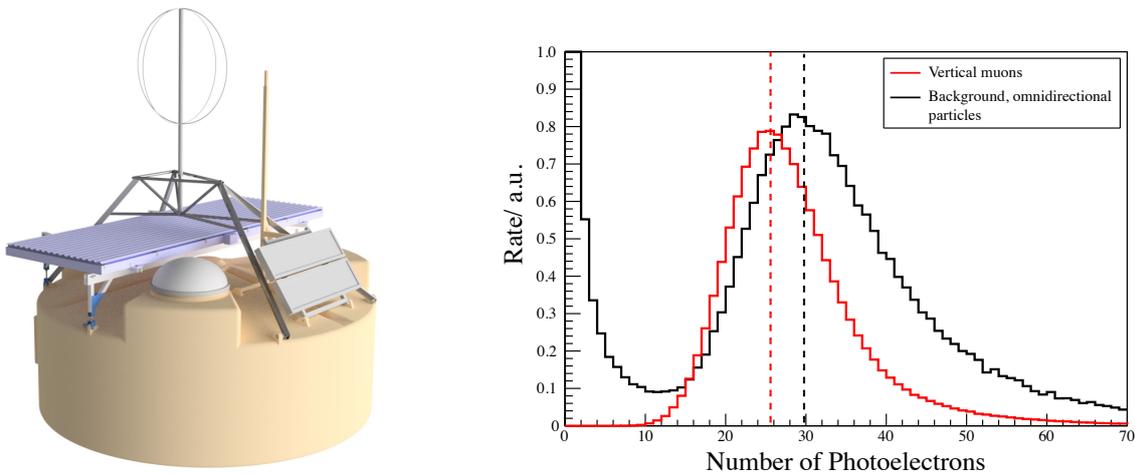
Figure 1: *Left:* Depiction of an AugerPrime surface detector station comprised of a water-Cherenkov detector (bottom), Scintillator Surface Detector (middle), and radio antenna (top). *Right:* Distributions of charge measured by the SSD from the simulated omni-directional flux of background particles (black) and uniformly-distributed, vertical muons (red).

3. Reconstruction at the level of the station

Prior to incorporating SSD measurements in the reconstruction of the properties of an air shower, signals measured by individual detectors must be calibrated to a common standard and the time range of signals pertinent to the shower in question must be determined. Additionally, the uncertainty in the measured signals must be quantified.

Calibration The signals measured by SSDs participating in an event are converted from ADC counts to the reference unit of a vertical Minimum Ionizing Particle, referred to as a "MIP" for short in congruence with standard nomenclature. The MIP is defined here as the peak of the distribution of charges produced by vertical, 1 GeV muons uniformly incident across the active surface of the SSD. To determine the conversion factor for individual detectors, the distribution of charges produced in an SSD by the omnidirectional background flux of particles is monitored at intervals of 61 s. The peak in this distribution is directly related to the MIP by a factor estimated to be 1.16 ± 0.02 using simulations of the SSD response to the simulated flux of background particles at the Observatory (see Fig. 1 (*right*)). At present, the trigger used to build calibration histograms for the SSD is that used for the WCD "VEM" calibration histograms [8]. This choice of trigger influences the angular distribution of particles contributing to the SSD charge histogram and also imposes an energy threshold. The effect of this choice in trigger is visible in simulations on the low end of the charge distribution; however, no significant impact on the position of the peak of the distribution, and hence the conversion factor to MIP, has been observed. An in situ measurement of this factor, analogous to that performed for the WCD [9], is planned.

Integration window Determining the portion of a trace relevant to the shower in question is important both in determining the arrival time of the shower front as well as in determining its thickness. It is desirable to integrate over a time window that encompasses all signals relating to the shower whilst excluding so-called "accidental" signals from background showers that are not
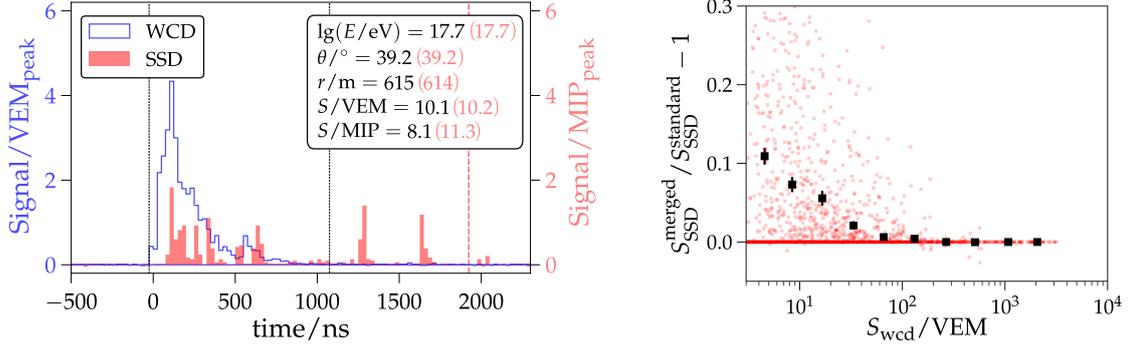
Figure 2: *Left:* Sample traces measured by a WCD and SSD. The black, dashed vertical lines indicate the integration window as determined from traces of the three WCD PMTs alone. Merging of the signal windows independently determined for the WCD and SSD PMTs resulted in an integration window with a stop bin (dashed pink line) approximately 800 ns later. *Right:* Relative increase of the SSD signal as calculated with the merged integration window as compared with the window determined from the PMTs of the WCD alone.

causally connected to the event. An elaborate algorithm determining whether adjacent segments of traces with signal are causally connected was developed for application to the traces measured by the three WCD PMTs [7]. At present, this algorithm is applied as is to the additional trace of the SSD PMT. If the segment of the SSD trace determined to have signal related to the shower in question has its start prior to or its finish after the integration window of the WCD, the merged window from the SSD and WCD PMTs is used to calculate the SSD signal. Signals significantly after those of the WCD are observed in SSD traces, examples of which are shown in Fig. 2 (*left*), and SSD signals calculated using the merged window are on average approximately 10% larger than when using the window determined using exclusively measurements of the WCD PMTs for measurements where the WCD signal is less than 10 VEM (see Fig. 2 (*right*)). The magnitude of these additional contributions to the SSD signal decrease relative to the total signal with increasing signal size and amount to less than 1% on average for measurements where the WCD signal is greater than 60 VEM. Studies on the impact of using the merged integration window to calculate the WCD signal were also performed to determine if the additional information from the SSD aids in picking up on sub-threshold signals in the WCD, but no significant changes were observed. The algorithms for the WCD making use only of the WCD PMTs were therefore kept for compatibility with WCD measurements prior to the *AugerPrime* era.

Uncertainties in signal measurement The signal measured by an SSD derives from a sample of the lateral distribution of particles at the ground and therefore has an associated uncertainty. Traditionally, this uncertainty is measured with so-called "multiplet" stations, which are two or more detectors separated by ∼10 m, which sample essentially the same position in the shower plane for a given shower. In the case of the SSD, for which measured showers were initially scarce, so-called *pseudo-doublets* were simulated. These consisted of pairs of stations, each at the same lateral distance of 1000 m in the shower plane and on laterally opposite sides of the shower axis (see Fig. 3 (*left*)). Two SSDs simulated at a distance of 10 m from one another could not be used to derive signal uncertainties as the thinning algorithms used in air shower simulations would result in a distortion
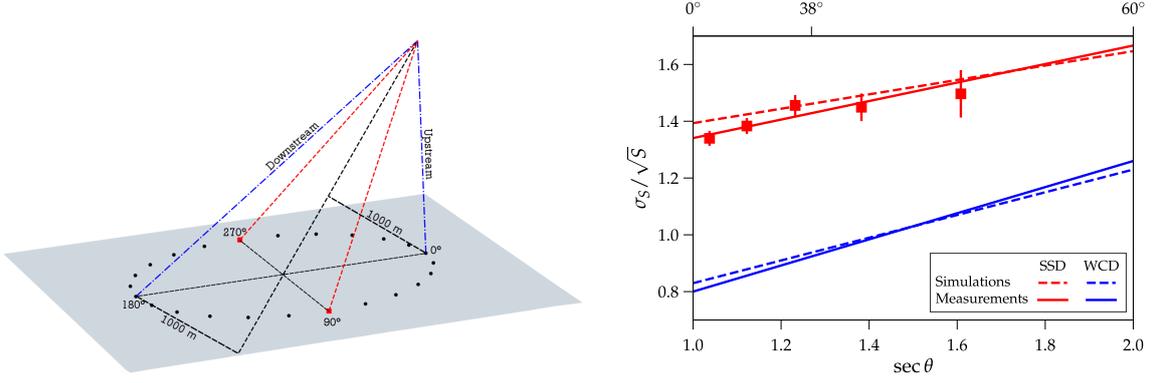
Figure 3: *Left:* Schematic depiction of a dense ring of stations at 1000 m from the shower axis. *Right:* Comparison of signal uncertainties derived from measurements and from simulations for the WCD and SSD.

of the fluctuations on small distance scales in the shower plane. This method of estimating signal uncertainties with pseudo-doublets was first tested with WCD simulations, where the resulting signal uncertainties were shown to be comparable to those measured with real doublet stations. In accordance with the underlying counting nature of scintillator detectors, the uncertainties in signals were shown to be proportional to the square root of the signal, with the constant of proportionality observable in Fig. 3 (*right*) as a function of zenith angle. Also shown in Fig. 3 (*right*) is a first derivation of a signal uncertainty model using in situ SSD doublet measurements. Although the quantity of doublet measurements is still limited, particularly at high energies and large zenith angles, the measured and simulated uncertainties appear to be roughly in agreement. As with the WCDs, the signal uncertainty of the SSDs σ_S is modeled with a Poisson-like parameterization, $\sigma_S^2 = f_S^2(\theta)\,S$, where $f_S(\theta) = a + b\sec\theta$. Due to the nature of Poisson fluctuations, the relative uncertainty of signals decreases with increasing signal magnitude and amounts to only a few percent for signals measured within a few hundred meters from the shower axis.

4. Reconstruction of the shower size

As the WCDs and SSDs differ in their sensitivity to the different particle types, a shower-size estimate from each detector would permit the deconvolution of the magnitudes of the muonic and electromagnetic components of air showers. In the following, work towards reconstruction of a shower-size estimator $S(1000)_{\mathrm{ssd}}$, defined as the SSD signal at 1000 m from the shower axis, is described.

Shower geometry Algorithms using measurements of the surface detector of the Observatory have hitherto made use of both the start times and signal magnitudes of triggered WCDs in order to reconstruct the shower geometry (i.e. the arrival direction and core position) [7]. The start times, which serve as estimates of the arrival time of the shower front at a station, provide the bulk of the information for reconstructing the axis of air showers, and the signal magnitudes, particularly their fall-off with distance, help constrain the position of the core. Close to the shower axis, where there are many particles, the resolution of the station GPS dominates the start time uncertainty and at large distances from the shower axis, sampling fluctuations dominate. Given the larger size
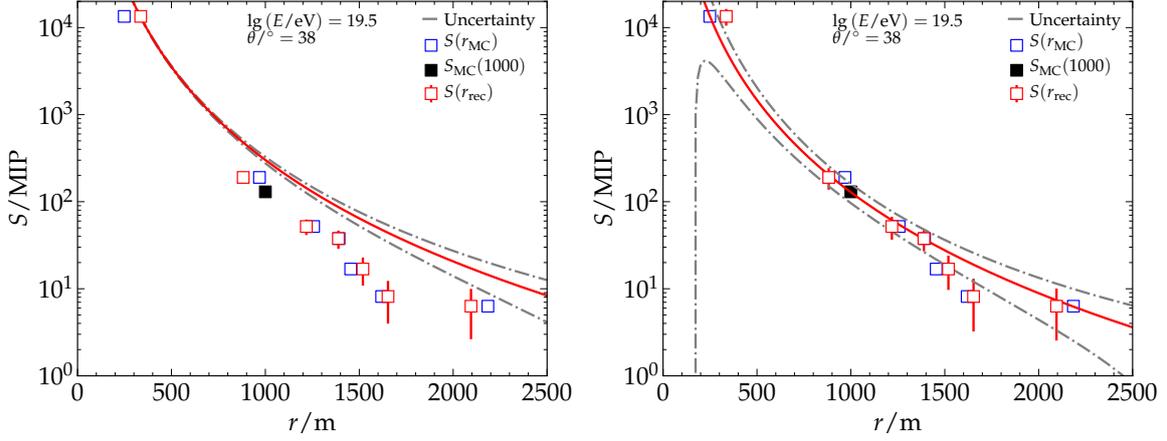
Figure 4: *Left:* Lateral distribution of SSD signals for a simulated event. Both the true (blue squares) and reconstructed (red squares) distances of stations from the shower axis are shown. The dashed grey lines indicate the uncertainties associated with the predicted signals according to the model of sampling fluctuations given in Section 3. Here, uncertainties in the core have not yet been taken into account. *Right:* The same event, but where core uncertainties have been propagated into the signal.

of the WCD, and accordingly smaller sampling fluctuations than those of the SSD, improvements to the determination of timing of the passage of the shower front are not expected to be dramatic with the incorporation of SSD measurements. With respect to improving resolution and bias in the determination of the position of the shower core, it has yet to be clearly determined the extent to which SSD measurements will aid. Azimuthal asymmetries in the signals measured in the shower plane, which differ in magnitude between the two detectors, must be well understood for their joint use in a combined likelihood, lest they result in systematic error in the reconstructed position of the core.

At present, the well-studied reconstruction of shower geometry using only the time and signal information of the WCD [7] is adopted as is for fitting the lateral distribution of SSD signals. Since the distance of a given SSD from the shower axis depends on the position of the reconstructed core, the fit of the lateral distribution function (LDF) must take into account the uncertainties therein. The LDF rises very steeply near the shower core and thus any error in determination of the distance to the shower axis results in a change in the predicted signal that significantly exceeds the uncertainty on the measured signal. Left unaccounted for, this can result in a severely mis-reconstructed LDF and hence a poorly reconstructed $S(1000)_{\text{ssd}}$. For an example, see Fig. 4 (*left*).

Considering all quantities relative to the true core position, it is assumed that the reconstructed core position (x_r, y_r), is a two-dimensional normal distribution, i.e. x_r and y_r are independent and (normally) distributed as $\mathcal{N}(x_r; 0, \sigma_c)$ and $\mathcal{N}(y_r; 0, \sigma_c)$, respectively. The true distance r of a station located at coordinates (x, y) from the core is given by $r^2 = x^2 + y^2$. The reconstructed distance r_r is therefore given by $r_r^2 = (x - x_r)^2 + (y - y_r)^2$. When $r \gg \sigma_c$, the reconstructed distance follows a normal distribution $\mathcal{N}(r_r; r, \sigma_c)$ and the uncertainty of the distance, $\delta r \sim r - r_r$, is thus equal to σ_c. For stations close to the core, the distribution of r_r is characterized by a Rayleigh distribution $\mathcal{R}(r; \sigma_c) = \frac{r}{\sigma_c^2} \exp(-r^2/2\sigma_c^2)$ defined for $r \geq 0$. The standard deviation of this distribution is smaller, namely $\delta r = \rho \, \sigma_c$, where $\rho = \sqrt{2 - \pi/2} \approx 0.655$. For stations at distances of $r \ll 2\sigma_c$ to

the core, the uncertainty δr thus starts at the Rayleigh value $\rho\sigma_c$ and quickly approaches the value σ_c at larger distances, where the vast majority of measurements with the SSD occur. The uncertainty of the core position σ_c is dependent on zenith angle and shower size and has been parameterized. For the 1500 m array, it can be as large as 100 m, which means that for stations at distances of a few hundred meters from the shower axis, where the LDF is very steep, the core resolution is on the order of the distance itself. The core resolution is propagated into the SSD signal using Gaussian error propagation. Since it is independent of the SSD signal, it is added in quadrature with the sampling fluctuations. Performing this propagation of core uncertainties significantly reduces outliers in the reconstructed $S(1000)_{ssd}$ and improves the resolution by a factor of ~2.5. Fig. 4 (*right*) shows the same sample event as in Fig. 4 (*left*), but where core uncertainties have been propagated.

Lateral distribution function   The signal as a function of the distance to the shower axis is expressed as $S(r) = S(r_{opt}) f_{NKG}(r)$ where f_{NKG} is a modified NKG-like function

$$f_{NKG}(r) = \left(\frac{r}{r_{opt}}\right)^{\beta} \left(\frac{r + r_s}{r_{opt} + r_s}\right)^{\beta+\gamma} . \tag{1}$$

Since the optimum distance r_{opt} at which to determine the shower size largely depends on detector spacing and array geometry [10] and since the SSDs are co-located with the WCDs, an r_{opt} of 1000 m (the same as for the WCD) was adopted for the SSD. Pending further study, the same value of 700 m was also chosen for r_s. Since most events have a multiplicity of triggering stations with an SSD signal greater than 1 MIP of only around three, the shape of the LDF is parameterized and only the shower size $S(1000)_{ssd}$ is fit. At $10^{19.5}$ eV, most events will have more than 10 SSDs with a signal greater than 1 MIP, leaving the possibility to additionally fit the LDF slope in the future. Additional measurements are required to perform a reasonable parameterization of the LDF shape for all zenith angles and shower sizes of interest. In the meantime, an initial parameterization of the shape parameters β and γ has been performed using simulated showers and the Monte-Carlo geometry. Both β and γ are parameterized linearly in $\lg(S(1000)_{ssd})$ and quadratically in $\sec\theta$.

Fit   For any given event, a maximum-likelihood fit of the SSD LDF is performed. The likelihood function consists of the product of probabilities of observing the measured signal S given an expected signal $\hat{S}$, that is $\mathcal{L} = \prod_{i=1}^{N} p(S_i|\hat{S}_i, \sigma_i)$, where $p(S|\hat{S}, \sigma)$ is the probability density function chosen to be either a truncated Gaussian or, after reformulation in terms of effective particle numbers, a Poisson distribution. For signals larger than a few MIP, both choices yield nearly identical probability distributions that are well approximated with a Gaussian whose width is defined by the model of sampling fluctuations described in Section 3. Both choices were explored and neither was clearly shown to describe small signals, where the choice is relevant, better than the other. Study of the uncertainties associated with such small signals is complicated by their proximity to the trigger threshold of the WCD. Pending further study and due to systematic uncertainties associated with the current treatment of small signals, they are currently excluded from the reconstruction. A maximum distance r_{cut} is empirically parameterized as second order polynomial of $S(1000)_{wcd}$ and $\sec\theta$ to ensure that 95% of SSDs at distances of r_{cut} have a signal of least 1 MIP.

Application   A sublime example event measured shortly after the commissioning of the first production design SSDs is shown in Fig. 5 (*left*). Residuals with respect to the fitted LDF for measurements of deployed SSDs are shown in Fig. 5 (*right*).
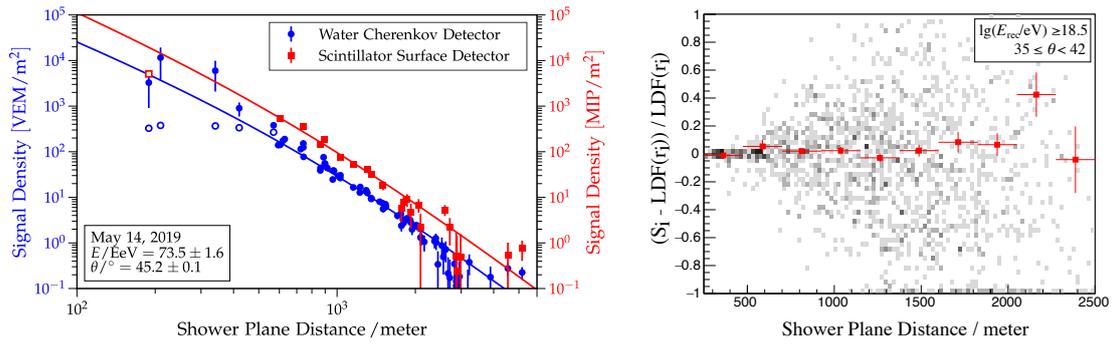
Figure 5: *Left:* Sample high-energy event measured in the SSD pre-production array. Although the reconstruction was performed using only stations in the 1500 m array, additional measurements of stations in the denser arrays in this region of the Observatory are also displayed. *Right:* Residuals with respect to the fitted LDF for signals measured by deployed SSDs.

5. Conclusions and outlook

We have provided a brief overview of the current status of algorithms developed to reconstruct a shower-size estimator from measurements by the SSDs of AugerPrime as an observable complementary to the shower-size estimator reconstructed by the WCDs. Moving towards the reconstruction of primary mass, work on the deconvolution of the contributions of the electromagnetic and muonic shower components to the reconstructed shower-size estimators is currently on-going. More sophisticated algorithms making use not only of signal magnitudes but also the time structure of traces are currently also being developed. Some make extensive use of the principles of air shower universality and others apply machine learning techniques. For the classical reconstruction methods presented here, a number of areas of improvement also remain. The optimal distance or distances with respect to sensitivity to primary mass, the search for a more appropriate LDF function to match the response of the SSD, and the formulation of a combined fit of WCD and SSD lateral distributions in the same likelihood are a just a few such areas. That the SSD and WCD measurements are co-located and therefore sample the lateral distribution at the exact same position in the shower plane is a fact that also has yet to be fully exploited.

References

[1] A. Aab et al. [Pierre Auger Coll.], *Phys. Rev. D* **90** (2014) 122005 [1409.4809]

[2] A. Aab et al. [Pierre Auger Coll.], [1604.03637]

[3] A. Castellina et al. [for the Pierre Auger Coll.], *Proc. Ultra High Energy Cosmic Rays Conf., Paris, France (2018)* EPJ Web Conf. **210** (2019) 06002, [1905.04472].

[4] I. Allekotte et al. [Pierre Auger Coll.], *Nucl. Instrum. Meth. A* **586** (2008) 409–420 [0712.2832]

[5] R. Šmída et al. [for the Pierre Auger Coll.], *Proc. 35th Int. Cosmic Ray Conf., Busan, Korea (2017)*, PoS(ICRC2017)390, [1708.06592].

[6] G. Cataldi [for the Pierre Auger Coll.], these proceedings.

[7] A. Aab et al. [Pierre Auger Coll.], *JINST* **15** (2020) P10021 [2007.09035]

[8] X. Bertou et al. [Pierre Auger Coll.], *Nucl. Instrum. Meth. A* **568** (2006) 839–846 [2102.01656]

[9] A. Aab et al. [Pierre Auger Coll.], *JINST* **15** (2020) P09002 [2007.04139]

[10] D. Newton et al., *Astropart. Phys.* **26** (2007) 414–419 [astro-ph/0608118]

The Pierre Auger Collaboration

P. Abreu[72], M. Aglietta[54,52], J.M. Albury[13], I. Allekotte[1], A. Almela[8,12], J. Alvarez-Muñiz[79], R. Alves Batista[80], G.A. Anastasi[63,52], L. Anchordoqui[87], B. Andrada[8], S. Andringa[72], C. Aramo[50], P.R. Araújo Ferreira[42], J. C. Arteaga Velázquez[67], H. Asorey[8], P. Assis[72], G. Avila[11], A.M. Badescu[75], A. Bakalova[32], A. Balaceanu[73], F. Barbato[45,46], R.J. Barreira Luz[72], K.H. Becker[38], J.A. Bellido[13,69], C. Berat[36], M.E. Bertaina[63,52], X. Bertou[1], P.L. Biermann[b], V. Binet[6], K. Bismark[39,8], T. Bister[42], J. Biteau[37], J. Blazek[32], C. Bleve[36], M. Boháčová[32], D. Boncioli[57,46], C. Bonifazi[9,26], L. Bonneau Arbeletche[21], N. Borodai[70], A.M. Botti[8], J. Brack[d], T. Bretz[42], P.G. Brichetto Orchera[8], F.L. Briechle[42], P. Buchholz[44], A. Bueno[78], S. Buitink[15], M. Buscemi[47], M. Büsken[39,8], K.S. Caballero-Mora[66], L. Caccianiga[59,49], F. Canfora[80,81], I. Caracas[38], J.M. Carceller[78], R. Caruso[58,47], A. Castellina[54,52], F. Catalani[19], G. Cataldi[48], L. Cazon[72], M. Cerda[10], J.A. Chinellato[22], J. Chudoba[32], L. Chytka[33], R.W. Clay[13], A.C. Cobos Cerutti[7], R. Colalillo[60,50], A. Coleman[93], M.R. Coluccia[48], R. Conceição[72], A. Condorelli[45,46], G. Consolati[49,55], F. Contreras[11], F. Convenga[56,48], D. Correia dos Santos[28], C.E. Covault[85], S. Dasso[5,3], K. Daumiller[41], B.R. Dawson[13], J.A. Day[13], R.M. de Almeida[28], J. de Jesús[8,41], S.J. de Jong[80,81], G. De Mauro[80,81], J.R.T. de Mello Neto[26,27], I. De Mitri[45,46], J. de Oliveira[18], D. de Oliveira Franco[22], F. de Palma[56,48], V. de Souza[20], E. De Vito[56,48], M. del Río[11], O. Deligny[34], L. Deval[41,8], A. di Matteo[52], C. Dobrigkeit[22], J.C. D'Olivo[68], L.M. Domingues Mendes[72], R.C. dos Anjos[25], D. dos Santos[28], M.T. Dova[4], J. Ebr[32], R. Engel[39,41], I. Epicoco[56,48], M. Erdmann[42], C.O. Escobar[a], A. Etchegoyen[8,12], H. Falcke[80,82,81], J. Farmer[92], G. Farrar[90], A.C. Fauth[22], N. Fazzini[a], F. Feldbusch[40], F. Fenu[54,52], B. Fick[89], J.M. Figueira[8], A. Filipčič[77,76], T. Fitoussi[41], T. Fodran[80], M.M. Freire[6], T. Fujii[92,e], A. Fuster[8,12], C. Galea[80], C. Galelli[59,49], B. García[7], A.L. Garcia Vegas[42], H. Gemmeke[40], F. Gesualdi[8,41], A. Gherghel-Lascu[73], P.L. Ghia[34], U. Giaccari[80], M. Giammarchi[49], J. Glombitza[42], F. Gobbi[10], F. Gollan[8], G. Golup[1], M. Gómez Berisso[1], P.F. Gómez Vitale[11], J.P. Gongora[11], J.M. González[1], N. González[14], I. Goos[1,41], D. Góra[70], A. Gorgi[54,52], M. Gottowik[38], T.D. Grubb[13], F. Guarino[60,50], G.P. Guedes[23], E. Guido[52,63], S. Hahn[41,8], P. Hamal[32], M.R. Hampel[8], P. Hansen[4], D. Harari[1], V.M. Harvey[13], A. Haungs[41], T. Hebbeker[42], D. Heck[41], G.C. Hill[13], C. Hojvat[a], J.R. Hörandel[80,81], P. Horvath[33], M. Hrabovský[33], T. Huege[41,15], A. Insolia[58,47], P.G. Isar[74], P. Janecek[32], J.A. Johnsen[86], J. Jurysek[32], A. Kääpä[38], K.H. Kampert[38], N. Karastathis[41], B. Keilhauer[41], J. Kemp[42], A. Khakurdikar[80], V.V. Kizakke Covilakam[8,41], H.O. Klages[41], M. Kleifges[40], J. Kleinfeller[10], M. Köpke[39], N. Kunka[40], B.L. Lago[17], R.G. Lang[20], N. Langner[42], M.A. Leigui de Oliveira[24], V. Lenok[41], A. Letessier-Selvon[35], I. Lhenry-Yvon[34], D. Lo Presti[58,47], L. Lopes[72], R. López[64], L. Lu[94], Q. Luce[39], J.P. Lundquist[76], A. Machado Payeras[22], G. Mancarella[56,48], D. Mandat[32], B.C. Manning[13], J. Manshanden[43], P. Mantsch[a], S. Marafico[34], A.G. Mariazzi[4], I.C. Mariş[14], G. Marsella[61,47], D. Martello[56,48], S. Martinelli[41,8], O. Martínez Bravo[64], M. Mastrodicasa[57,46], H.J. Mathes[41], J. Matthews[88], G. Matthiae[62,51], E. Mayotte[38], P.O. Mazur[a], G. Medina-Tanco[68], D. Melo[8], A. Menshikov[40], K.-D. Merenda[86], S. Michal[33], M.I. Micheletti[6], L. Miramonti[59,49], S. Mollerach[1], F. Montanet[36], C. Morello[54,52], M. Mostafá[91], A.L. Müller[8], M.A. Muller[22], K. Mulrey[15], R. Mussa[52], M. Muzio[90], W.M. Namasaka[38], A. Nasr-Esfahani[38], L. Nellen[68], M. Niculescu-Oglinzanu[73], M. Niechciol[44], D. Nitz[89], D. Nosek[31], V. Novotny[31], L. Nožka[33], A Nucita[56,48], L.A. Núñez[30], M. Palatka[32], J. Pallotta[2], P. Papenbreer[38], G. Parente[79], A. Parra[64], J. Pawlowsky[38], M. Pech[32], F. Pedreira[79], J. Pękala[70], R. Pelayo[65], J. Peña-Rodriguez[30], E.E. Pereira Martins[39,8], J. Perez Armand[21], C. Pérez Bertolli[8,41], M. Perlin[8,41], L. Perrone[56,48], S. Petrera[45,46], T. Pierog[41], M. Pimenta[72], V. Pirronello[58,47], M. Platino[8], B. Pont[80], M. Pothast[81,80], P. Privitera[92], M. Prouza[32], A. Puyleart[89], S. Querchfeld[38], J. Rautenberg[38], D. Ravignani[8], M. Reininghaus[41,8], J. Ridky[32], F. Riehn[72], M. Risse[44], V. Rizi[57,46], W. Rodrigues de Carvalho[21], J. Rodriguez Rojo[11], M.J. Roncoroni[8], S. Rossoni[43], M. Roth[41], E. Roulet[1], A.C. Rovero[5], P. Ruehl[44], A. Saftoiu[73], F. Salamida[57,46], H. Salazar[64], G. Salina[51], J.D. Sanabria Gomez[30], F. Sánchez[8], E.M. Santos[21], E. Santos[32], F. Sarazin[86], R. Sarmento[72], C. Sarmiento-Cano[8], R. Sato[11],

9

P. Savina[56,48,34,94], C.M. Schäfer[41], V. Scherini[56,48], H. Schieler[41], M. Schimassek[39,8], M. Schimp[38], F. Schlüter[41,8], D. Schmidt[39], O. Scholten[84,15], P. Schovánek[32], F.G. Schröder[93,41], S. Schröder[38], J. Schulte[42], S.J. Sciutto[4], M. Scornavacche[8,41], A. Segreto[53,47], S. Sehgal[38], R.C. Shellard[16], G. Sigl[43], G. Silli[8,41], O. Sima[73,f], R. Šmída[92], P. Sommers[91], J.F. Soriano[87], J. Souchard[36], R. Squartini[10], M. Stadelmaier[41,8], D. Stanca[73], S. Stanič[76], J. Stasielak[70], P. Stassi[36], A. Streich[39,8], M. Suárez-Durán[14], T. Sudholz[13], T. Suomijärvi[37], A.D. Supanitsky[8], Z. Szadkowski[71], A. Tapia[29], C. Taricco[63,52], C. Timmermans[81,80], O. Tkachenko[41], P. Tobiska[32], C.J. Todero Peixoto[19], B. Tomé[72], Z. Torrès[36], A. Travaini[10], P. Travnicek[32], C. Trimarelli[57,46], M. Tueros[4], R. Ulrich[41], M. Unger[41], L. Vaclavek[33], M. Vacula[33], J.F. Valdés Galicia[68], L. Valore[60,50], E. Varela[64], A. Vásquez-Ramírez[30], D. Veberič[41], C. Ventura[27], I.D. Vergara Quispe[4], V. Verzi[51], J. Vicha[32], J. Vink[83], S. Vorobiov[76], H. Wahlberg[4], C. Watanabe[26], A.A. Watson[c], M. Weber[40], A. Weindl[41], L. Wiencke[86], H. Wilczyński[70], M. Wirtz[42], D. Wittkowski[38], B. Wundheiler[8], A. Yushkov[32], O. Zapparrata[14], E. Zas[79], D. Zavrtanik[76,77], M. Zavrtanik[77,76], L. Zehrer[76]

———————— • ————————

[1] Centro Atómico Bariloche and Instituto Balseiro (CNEA-UNCuyo-CONICET), San Carlos de Bariloche, Argentina

[2] Centro de Investigaciones en Láseres y Aplicaciones, CITEDEF and CONICET, Villa Martelli, Argentina

[3] Departamento de Física and Departamento de Ciencias de la Atmósfera y los Océanos, FCEyN, Universidad de Buenos Aires and CONICET, Buenos Aires, Argentina

[4] IFLP, Universidad Nacional de La Plata and CONICET, La Plata, Argentina

[5] Instituto de Astronomía y Física del Espacio (IAFE, CONICET-UBA), Buenos Aires, Argentina

[6] Instituto de Física de Rosario (IFIR) – CONICET/U.N.R. and Facultad de Ciencias Bioquímicas y Farmacéuticas U.N.R., Rosario, Argentina

[7] Instituto de Tecnologías en Detección y Astropartículas (CNEA, CONICET, UNSAM), and Universidad Tecnológica Nacional – Facultad Regional Mendoza (CONICET/CNEA), Mendoza, Argentina

[8] Instituto de Tecnologías en Detección y Astropartículas (CNEA, CONICET, UNSAM), Buenos Aires, Argentina

[9] International Center of Advanced Studies and Instituto de Ciencias Físicas, ECyT-UNSAM and CONICET, Campus Miguelete – San Martín, Buenos Aires, Argentina

[10] Observatorio Pierre Auger, Malargüe, Argentina

[11] Observatorio Pierre Auger and Comisión Nacional de Energía Atómica, Malargüe, Argentina

[12] Universidad Tecnológica Nacional – Facultad Regional Buenos Aires, Buenos Aires, Argentina

[13] University of Adelaide, Adelaide, S.A., Australia

[14] Université Libre de Bruxelles (ULB), Brussels, Belgium

[15] Vrije Universiteit Brussels, Brussels, Belgium

[16] Centro Brasileiro de Pesquisas Fisicas, Rio de Janeiro, RJ, Brazil

[17] Centro Federal de Educação Tecnológica Celso Suckow da Fonseca, Nova Friburgo, Brazil

[18] Instituto Federal de Educação, Ciência e Tecnologia do Rio de Janeiro (IFRJ), Brazil

[19] Universidade de São Paulo, Escola de Engenharia de Lorena, Lorena, SP, Brazil

[20] Universidade de São Paulo, Instituto de Física de São Carlos, São Carlos, SP, Brazil

[21] Universidade de São Paulo, Instituto de Física, São Paulo, SP, Brazil

[22] Universidade Estadual de Campinas, IFGW, Campinas, SP, Brazil

[23] Universidade Estadual de Feira de Santana, Feira de Santana, Brazil

[24] Universidade Federal do ABC, Santo André, SP, Brazil

[25] Universidade Federal do Paraná, Setor Palotina, Palotina, Brazil

[26] Universidade Federal do Rio de Janeiro, Instituto de Física, Rio de Janeiro, RJ, Brazil

[27] Universidade Federal do Rio de Janeiro (UFRJ), Observatório do Valongo, Rio de Janeiro, RJ, Brazil

[28] Universidade Federal Fluminense, EEIMVR, Volta Redonda, RJ, Brazil

[29] Universidad de Medellín, Medellín, Colombia

[30] Universidad Industrial de Santander, Bucaramanga, Colombia

[31] Charles University, Faculty of Mathematics and Physics, Institute of Particle and Nuclear Physics, Prague, Czech Republic

[32] Institute of Physics of the Czech Academy of Sciences, Prague, Czech Republic

[33] Palacky University, RCPTM, Olomouc, Czech Republic

[34] CNRS/IN2P3, IJCLab, Université Paris-Saclay, Orsay, France

[35] Laboratoire de Physique Nucléaire et de Hautes Energies (LPNHE), Sorbonne Université, Université de Paris, CNRS-IN2P3, Paris, France

[36] Univ. Grenoble Alpes, CNRS, Grenoble Institute of Engineering Univ. Grenoble Alpes, LPSC-IN2P3, 38000 Grenoble, France

[37] Université Paris-Saclay, CNRS/IN2P3, IJCLab, Orsay, France

[38] Bergische Universität Wuppertal, Department of Physics, Wuppertal, Germany

[39] Karlsruhe Institute of Technology (KIT), Institute for Experimental Particle Physics, Karlsruhe, Germany

[40] Karlsruhe Institute of Technology (KIT), Institut für Prozessdatenverarbeitung und Elektronik, Karlsruhe, Germany

[41] Karlsruhe Institute of Technology (KIT), Institute for Astroparticle Physics, Karlsruhe, Germany

[42] RWTH Aachen University, III. Physikalisches Institut A, Aachen, Germany

[43] Universität Hamburg, II. Institut für Theoretische Physik, Hamburg, Germany

[44] Universität Siegen, Department Physik – Experimentelle Teilchenphysik, Siegen, Germany

[45] Gran Sasso Science Institute, L'Aquila, Italy

[46] INFN Laboratori Nazionali del Gran Sasso, Assergi (L'Aquila), Italy

[47] INFN, Sezione di Catania, Catania, Italy

[48] INFN, Sezione di Lecce, Lecce, Italy

[49] INFN, Sezione di Milano, Milano, Italy

[50] INFN, Sezione di Napoli, Napoli, Italy

[51] INFN, Sezione di Roma "Tor Vergata", Roma, Italy

[52] INFN, Sezione di Torino, Torino, Italy

[53] Istituto di Astrofisica Spaziale e Fisica Cosmica di Palermo (INAF), Palermo, Italy

[54] Osservatorio Astrofisico di Torino (INAF), Torino, Italy

[55] Politecnico di Milano, Dipartimento di Scienze e Tecnologie Aerospaziali , Milano, Italy

[56] Università del Salento, Dipartimento di Matematica e Fisica "E. De Giorgi", Lecce, Italy

[57] Università dell'Aquila, Dipartimento di Scienze Fisiche e Chimiche, L'Aquila, Italy

[58] Università di Catania, Dipartimento di Fisica e Astronomia, Catania, Italy

[59] Università di Milano, Dipartimento di Fisica, Milano, Italy

[60] Università di Napoli "Federico II", Dipartimento di Fisica "Ettore Pancini", Napoli, Italy

[61] Università di Palermo, Dipartimento di Fisica e Chimica "E. Segrè", Palermo, Italy

[62] Università di Roma "Tor Vergata", Dipartimento di Fisica, Roma, Italy

[63] Università Torino, Dipartimento di Fisica, Torino, Italy

[64] Benemérita Universidad Autónoma de Puebla, Puebla, México

[65] Unidad Profesional Interdisciplinaria en Ingeniería y Tecnologías Avanzadas del Instituto Politécnico Nacional (UPIITA-IPN), México, D.F., México

[66] Universidad Autónoma de Chiapas, Tuxtla Gutiérrez, Chiapas, México

[67] Universidad Michoacana de San Nicolás de Hidalgo, Morelia, Michoacán, México

[68] Universidad Nacional Autónoma de México, México, D.F., México

[69] Universidad Nacional de San Agustin de Arequipa, Facultad de Ciencias Naturales y Formales, Arequipa, Peru

[70] Institute of Nuclear Physics PAN, Krakow, Poland

[71] University of Łódź, Faculty of High-Energy Astrophysics,Łódź, Poland

[72] Laboratório de Instrumentação e Física Experimental de Partículas – LIP and Instituto Superior Técnico – IST, Universidade de Lisboa – UL, Lisboa, Portugal

[73] "Horia Hulubei" National Institute for Physics and Nuclear Engineering, Bucharest-Magurele, Romania

[74] Institute of Space Science, Bucharest-Magurele, Romania

[75] University Politehnica of Bucharest, Bucharest, Romania

[76] Center for Astrophysics and Cosmology (CAC), University of Nova Gorica, Nova Gorica, Slovenia

[77] Experimental Particle Physics Department, J. Stefan Institute, Ljubljana, Slovenia

[78] Universidad de Granada and C.A.F.P.E., Granada, Spain

[79] Instituto Galego de Física de Altas Enerxías (IGFAE), Universidade de Santiago de Compostela, Santiago de Compostela, Spain

[80] IMAPP, Radboud University Nijmegen, Nijmegen, The Netherlands

[81] Nationaal Instituut voor Kernfysica en Hoge Energie Fysica (NIKHEF), Science Park, Amsterdam, The Netherlands

[82] Stichting Astronomisch Onderzoek in Nederland (ASTRON), Dwingeloo, The Netherlands

[83] Universiteit van Amsterdam, Faculty of Science, Amsterdam, The Netherlands

[84] University of Groningen, Kapteyn Astronomical Institute, Groningen, The Netherlands

[85] Case Western Reserve University, Cleveland, OH, USA

[86] Colorado School of Mines, Golden, CO, USA

[87] Department of Physics and Astronomy, Lehman College, City University of New York, Bronx, NY, USA

[88] Louisiana State University, Baton Rouge, LA, USA

[89] Michigan Technological University, Houghton, MI, USA

[90] New York University, New York, NY, USA

[91] Pennsylvania State University, University Park, PA, USA

[92] University of Chicago, Enrico Fermi Institute, Chicago, IL, USA

[93] University of Delaware, Department of Physics and Astronomy, Bartol Research Institute, Newark, DE, USA

[94] University of Wisconsin-Madison, Department of Physics and WIPAC, Madison, WI, USA

———

[a] Fermi National Accelerator Laboratory, Fermilab, Batavia, IL, USA

[b] Max-Planck-Institut für Radioastronomie, Bonn, Germany

[c] School of Physics and Astronomy, University of Leeds, Leeds, United Kingdom

[d] Colorado State University, Fort Collins, CO, USA

[e] now at Hakubi Center for Advanced Research and Graduate School of Science, Kyoto University, Kyoto, Japan

[f] also at University of Bucharest, Physics Department, Bucharest, Romania